

## EFFECT OF ISOLATION DAMPING ON THE RESPONSE OF BASE ISOLATED STRUCTURE

Krishnamoorthy and Kiran K. Shetty\*  
Department of Civil Engineering, M.I.T., Manipal-576104, India

### ABSTRACT

The response of a multi-story space frame structure resting on non-linear base isolation system, subjected to bi-directional harmonic and seismic ground motions are studied. A four-storey space frame structure with consistent mass system having six degrees of freedom (three translations along x, y, z-axes and three rotations about these axes) at each node is considered for study. The effect of isolation damping and the excitation frequency on the response of a base isolated structure is investigated. The effect of excitation frequency, isolation period, superstructure time period and superstructure damping on the optimum isolation damping is also studied in this paper. It is shown that the above parameters have significant effects on optimum isolation damping. The response of isolated system is found to be less in comparison to the corresponding response without isolation system, implying that the isolation is effective in reducing acceleration and forces of the system.

**Keywords:** Non-linear base isolation system; time period of superstructure; isolation period; optimum isolation damping; superstructure damping, bi-directional ground motion

### 1. INTRODUCTION

Base isolation is an aseismic design approach in which the building is protected from the hazards of earthquake forces by a mechanism, which reduces the transmission of horizontal acceleration into the structure. One of the concepts to protect a building from the damaging effects of an earthquake is by introducing some type of support that isolates it from the shaking ground using specially designed bearing. These bearings are placed between the structure and its foundation. The most common type of this bearing consists of alternating layers of steel plates and hard rubber with and without a lead core. These bearings can carry the gravity load of the superstructure in normal way and simultaneously provide the horizontal flexibility necessary to shift its first mode natural frequency away from predominant frequency of the design earthquake motion. This results in the reduction of inertial forces and accelerations several times in the structure. But the additional flexibility necessary for shifting the first

---

\* Email-address of the corresponding author: kiran\_manoor @ yahoo.com (Kiran K. Shetty)

natural period induces large displacement at the isolation level, which must be reduced to an acceptable level by energy dissipation through the use of external dampers or introducing damping in bearing itself. The damping is desirable to keep the isolator displacement within limits in case of low frequency ground motion. However, the use of high damping rubber bearings increases the accelerations into the superstructure, which is undesirable for a structure containing sensitive equipments. Kelly [1] and Buckle and Mayes [2] carried out an extensive review on the historical developments of the many mechanisms that have been developed. Bhasker Rao and Jangid [3] conducted experimental and analytical study on the base isolated structure having only one lateral degree of freedom with lumped mass system. Tsai and Kelly [4] studied the influence of isolation damping on the seismic response of heavily damped base isolated shear building with lumped mass system. They found that when the damping ratio of the isolation system is beyond some level, increasing the isolation damping will enlarge the superstructure acceleration. Inaudi and Kelly [5] investigated the optimum isolation damping for minimum acceleration response of a base isolated shear structure with lumped mass system subjected to stationary random excitation. However, in their study they considered only a linear base isolation system. Jangid [6] investigated the optimum isolation damping for minimum acceleration of a base isolated structure with only one degree of freedom with lumped mass system subjected to earthquake ground excitation. In spite of several analytical studies carried out so far, the effect of excitation frequency, isolation period, superstructure time period and superstructure damping on the optimum isolation damping has not been given much importance. Also in most of the studies carried out, the behaviour of framed structure is modeled as shear building with one degree of freedom attached to the center of mass of each floor and the effect of other degrees of freedom on the response of structure are neglected. In this study the multi-story framed structure resting on non-linear rubber bearing is analysed by considering all the six degrees of freedom (three translations along x, y, z-axes and three rotations about these axes) at each node. Also in this study consistent mass is considered instead of lumped mass. The effect of isolation damping and the excitation frequency on the response of a base isolated structure is investigated. The effect of excitation frequency, isolation period, superstructure time period and superstructure damping on the optimum isolation damping is also studied in this paper. To study these effects a multi-story framed structure mounted on non-linear base isolation system is considered. The multi-story framed structure is subjected to bi-directional harmonic excitation frequencies, El Centro and Turkey earthquake ground motion. The response obtained from the analysis of the frame fixed at base is compared with the response obtained from the analysis of the frame isolated at base so as to study the effectiveness of base isolation.

## 2. ANALYSIS

### 2.1 Details of the analysis

The structure is divided into number of elements consisting of beams and columns. The beams and columns are modeled using two noded frame elements with six degrees of freedom at each node i.e., three translations along x, y and z-axes and three rotations about these axes. For each element, the stiffness matrix,  $k_s$ , consistent mass matrix,  $m_s$ , and

transformation matrix,  $t_s$ , is obtained. The mass matrix and the stiffness matrix of each element from local direction are transformed to global direction as proposed by Paz [7]. The mass matrix and the stiffness matrix of each element are assembled by direct stiffness method to get the overall mass matrix,  $M$ , and overall stiffness matrix,  $K$ , for the entire structure. Knowing the overall mass matrix,  $M$ , and overall stiffness matrix,  $K$ , the frequencies for the superstructure (fixed base structure) is obtained using simultaneous iteration method. The superstructure time period or fixed base time period is expressed as  $T_s = 2\pi / \omega_s$ , where  $\omega_s$  is the fundamental natural frequency of fixed base structure. The damping matrix for superstructure is obtained using Rayleigh's equation.  $C = \alpha M + \beta K$  where  $\alpha$  and  $\beta$  are the constants. These constants are determined using the damping ratio of the superstructure (which is assumed constant for all the modes) and the first two frequencies of fixed base structure. The overall dynamic equation of equilibrium for the entire structure can be expressed in matrix notations as

$$M \ddot{u} + C \dot{u} + K u = f(t) \quad (1)$$

where  $M$ ,  $C$  and  $K$  are the overall mass, damping, and stiffness matrices.  $\ddot{u}$ ,  $\dot{u}$ ,  $u$  are the relative acceleration, velocity and displacement vectors with respect to ground and  $f(t)$  is the nodal load vector.  $u = u_1, v_1, w_1, \theta_{x1}, \theta_{y1}, \theta_{z1}, u_2, v_2, w_2, \theta_{x2}, \theta_{y2}, \theta_{z2}, \dots, u_n, v_n, w_n, \theta_{xn}, \theta_{yn}, \theta_{zn}$  where  $n$  is the number of nodes.

The nodal load vector due to earthquake is obtained using the equation

$$f(t) = -M I \ddot{u}_g(t)$$

where  $M$  is the overall mass matrix,  $I$  is the influence vector,  $\ddot{u}_g(t)$  is the ground acceleration.

## 2.2 Modeling of isolation bearing

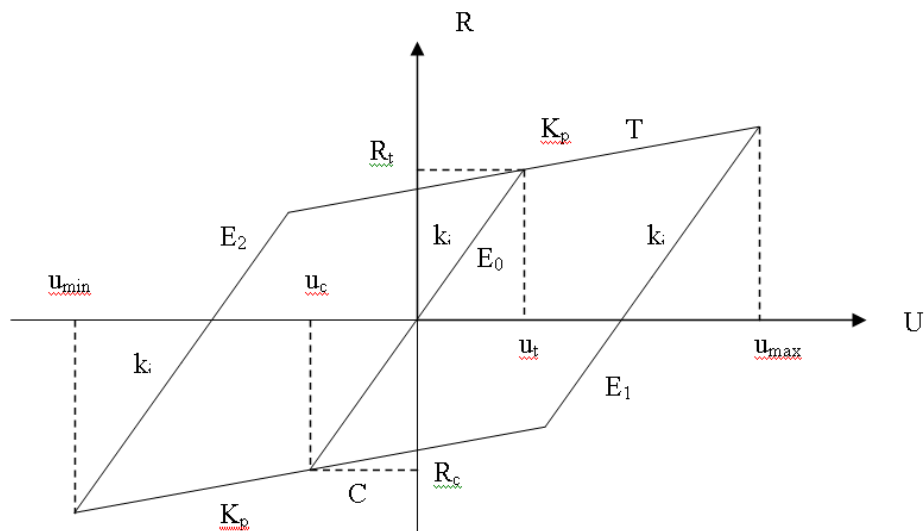


Figure 1. Bi-linear hysteretic model

The force deformation behaviour of the rubber bearing is modeled as non-linear, with two translational degrees of freedoms (x and z direction) at each node. The non-linear force deformation behaviour of the rubber bearing is modeled through the bi-linear hysteresis loop (Figure 1). The bearing passes through two phases 1) elastic phase and 2) plastic phase. Initially, as the load is applied, the bearing behaves elastically along the curve  $E_0$ . The displacement  $u_t$ , at which plastic behaviour in tension may be initiated and the displacement  $u_c$ , at which plastic behaviour in compression may be initiated are calculated, respectively, from

$$u_t = R_t / k_i$$

$$u_c = R_c / k_i$$

where  $R_t$  and  $R_c$  are the respective values of the forces, which produce yielding in tension and compression and  $k_i$ , the elastic stiffness of the bearing. The bearing will remain on the curve  $E_0$  as long as the displacement,  $u$  satisfies

$$u_c < u < u_t \quad (2)$$

If the displacement  $u$  increases to  $u_t$ , the bearing begins to behave plastically in tension along the curve T on Figure 1; it remain on the curve T as long as the velocity  $\dot{u} > 0$ . When  $\dot{u} < 0$ , the bearing reverse to elastic behaviour on a curve such as  $E_1$  with new yielding points given by

$$u_t = u_{\max}$$

$$u_c = u_{\max} - (R_t - R_c) / k_i ;$$

where  $u_{\max}$  is the maximum displacement along the curve T, which occurs when  $\dot{u} = 0$ ;

Conversely, if  $u$  decreases to  $u_c$ , the bearing begins a plastic behaviour in compression along curve C and it remains on this curve as long as  $\dot{u} < 0$ . The bearing returns to an elastic behaviour when the velocity again changes direction and  $\dot{u} > 0$ . In this case, the new yielding limits are given by

$$u_c = u_{\min}$$

$$u_t = u_{\min} + (R_t - R_c) / k_i$$

where  $u_{\min}$  is the minimum displacement along the curve C, which occurs when  $\dot{u} = 0$ . The same condition given by Eq. (2) is valid for the bearing to remain operating along any elastic segment such as  $E_0, E_1, E_2, \dots$  as shown in Figure 1. The damping for each bearing (in x and z direction) is calculated using the equation  $C_b = 2\zeta_b \sqrt{k_b M_t}$  where  $\zeta_b$  is the damping of the bearing,  $k_b$  is the stiffness of the bearing ( $k_b = k_i$ , in the elastic region and

$k_b = k_p = \eta k_i$ , in the plastic region;  $\eta$  = post-to-pre yield stiffness ratio) and  $M_t$  is the mass on the each bearing. The post-yield stiffness of the isolation system,  $k_p$  is generally designed in such a way to provide the specific value of the isolation period,  $T_b$ , expressed as  $T_b = 2\pi / \omega_b$  where  $\omega_b = \sqrt{k_p / M_t}$  is the base isolation frequency. The stiffness and the damping of the bearings are added at corresponding global degrees of freedom to the overall stiffness matrix and overall damping matrix of superstructure.

### 2.3 Determination of displacements and acceleration by Newmark method

To solve the equations of motion, the Newmark method is used. In this method, from the information at time  $t$  the response at time  $t + \Delta t$  is determined. Owing to its unconditional stability, the constant average acceleration scheme (with  $\beta = 1/4$  and  $\gamma = 1/2$ ) is adopted. The equation of motion (1) in incremental form can be written as

$$M \Delta \ddot{u}_i + C \Delta \dot{u}_i + K \Delta u_i = \Delta F_i \quad (3)$$

where  $\Delta$  denotes the variations of each parameters from  $t$  to time  $t + \Delta t$ , and index  $i$  indicates the  $i^{\text{th}}$  time step.

$$\Delta \dot{u}_i = \frac{2}{\Delta t} \Delta u_i - 2 \dot{u}_i \quad (4)$$

$$\Delta \ddot{u}_i = \frac{4}{\Delta t^2} \Delta u_i - \frac{4}{\Delta t} \dot{u}_i - 2 \ddot{u}_i \quad (5)$$

Substituting Eqs. (4) and (5) into Eq. (3) yields

$$\hat{K} \Delta u_i = \Delta \hat{F}_i \quad (6)$$

where

$$\hat{K} = K + \frac{2}{\Delta t} C + \frac{4}{\Delta t^2} M \quad (7)$$

$$\Delta \hat{F}_i = \Delta F_i + \left( \frac{4}{\Delta t} M + 2 C \right) \dot{u}_i + [2 M] \ddot{u}_i \quad (8)$$

By solving Eq. (6),  $\Delta u_i$  is determined and subsequent values of displacement and velocity at the beginning of step  $(i + 1)$  are calculated using Eq. (4) and the following two equations:

$$\begin{aligned} u_{i+1} &= u_i + \Delta u_i \\ \dot{u}_{i+1} &= \dot{u}_i + \Delta \dot{u}_i \end{aligned} \quad (9)$$

Accelerations are calculated from Eq.(1) to increase the accuracy and stability of

solutions.

#### 2.4 Determination of member forces

The displacement obtained at each node is assigned for each member. The forces in each member are then obtained by multiplying element stiffness matrix with the nodal displacement vector.

### 3. RESULTS AND DISCUSSIONS

#### 3.1 Studies on the performance of base isolated structure subjected to harmonic ground motion

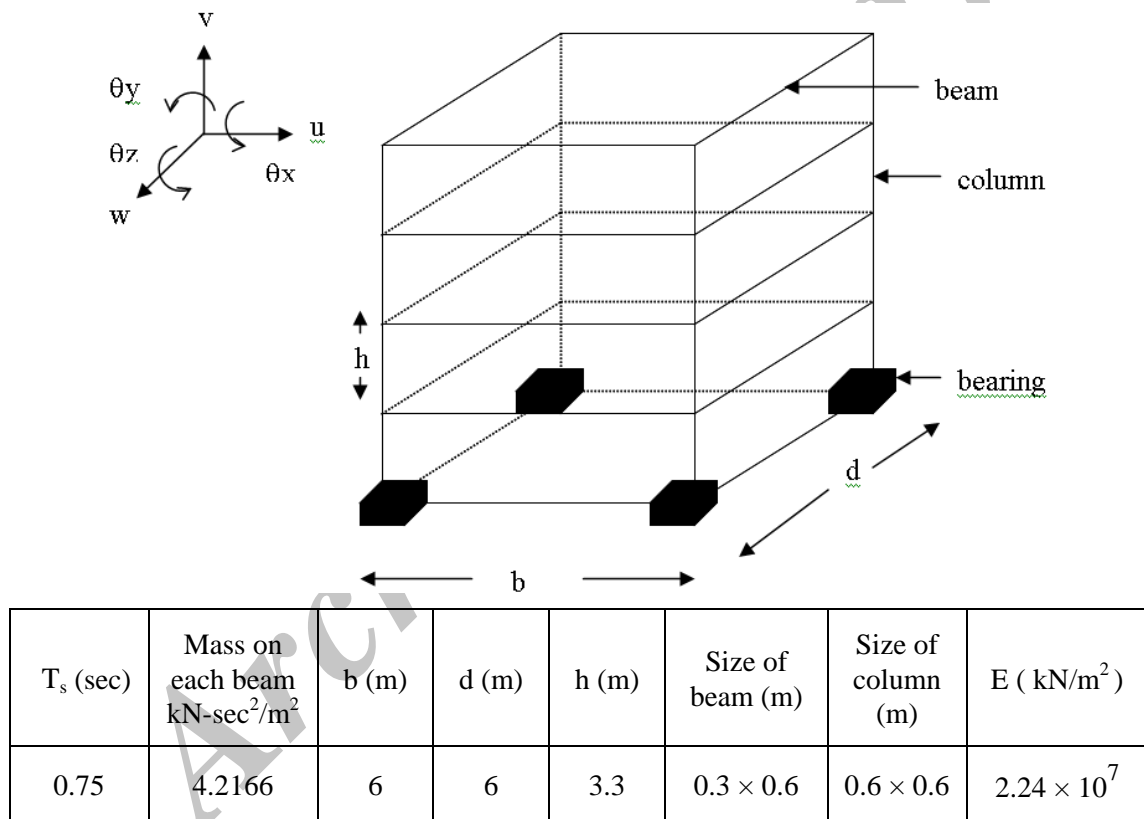
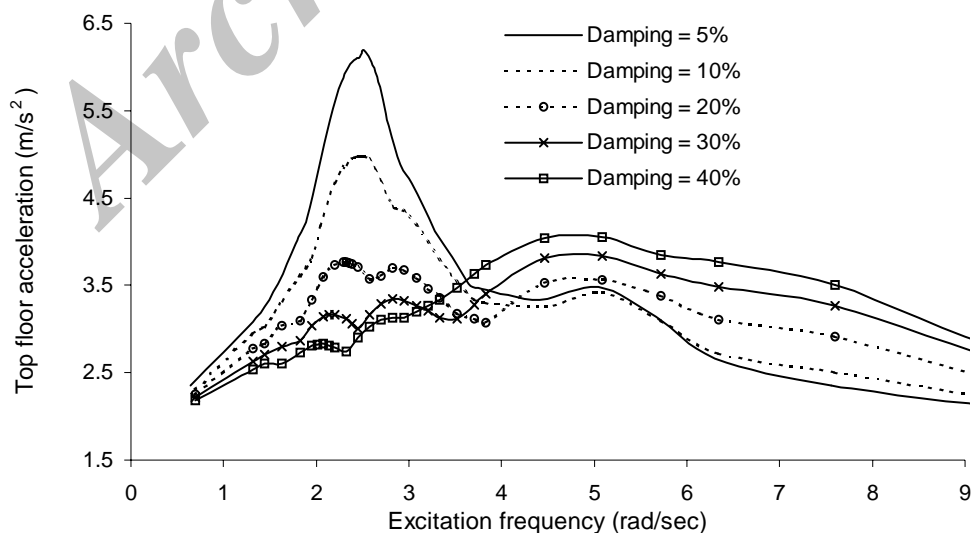


Figure 2. Four-storey space frame structure resting on non-linear rubber bearing

The response of a multi-storey space frame structure resting on non-linear base isolation system, subjected to bi-directional harmonic ground excitation equal to  $a_0 \sin(\omega t)$  (where  $a_0$  is equal to 20% of acceleration due to gravity) is studied. A four-storey space frame structure mounted on non-linear rubber bearing considered for the analysis is shown in Figure 2. The various material and geometric properties considered for the study are also shown in the same figure. The horizontal displacements, the top floor absolute acceleration and the forces in the members due to this loading are computed.

### 3.1.1 Effect of excitation frequency and isolation damping on response of base isolated structure

The effect of excitation frequency and isolation damping on the response of a four-story base isolated structure having fixed base time period is equal to 0.75 sec is studied. The yield displacement of the isolator is taken as 2.5cm. This value of yield displacement provides (For  $R_t = R_c = 0.08 W$  and  $\eta = 0.2$ ;  $W$  = total weight of the building) a time period of the bearing in lateral direction as 2.5 sec based on post-yield stiffness of the isolator. Damping is assumed to be 5% for superstructure. Figure 3 shows the variation of top floor acceleration, base shear and bending moment with excitation frequency for various values of isolation damping. It can be observed from Figure 3 that, the maximum acceleration occurs at 2.5 rad/sec upto an isolation damping of 20%. Further, for 30% and 40% isolation damping the maximum acceleration occurs at 5.2 rad/sec. However, the maximum base shear and maximum bending moment occurs at 2.5 rad/sec for all isolation damping. It can also be observed from Figure 3 that, upto an excitation frequency of 3 rad/sec the increase in isolation damping decreases the acceleration, base shear and the bending moment. In the region of excitation frequency between 3 rad/sec to 3.6 rad/sec, as the isolation damping increase from 5% to 30% the acceleration decreases and then it increases with the further increase in damping. However, the base shear and bending moment continuous to decrease with increase in isolation damping. Further, in the range of excitation frequency, 3.6 rad/sec  $< \omega < 4.2$  rad/sec, the acceleration decreases upto an isolation damping of 20% and then it increases with the further increase in damping. But the base shear and the bending moment decreases upto an isolation damping of 30% and then it also increases with increase in damping. In the region of excitation frequency between 4.2 rad/sec to 5.5 rad/sec, upto an isolation damping of 10% the acceleration decreases and then it increases with the further increase in damping. But the base shear and the bending moment decreases upto an isolation damping of 20% and then it also increases with increase in damping. Beyond an excitation frequency of 5.5 rad/sec, the increase in isolation damping increases the acceleration, base shear and the bending moment.



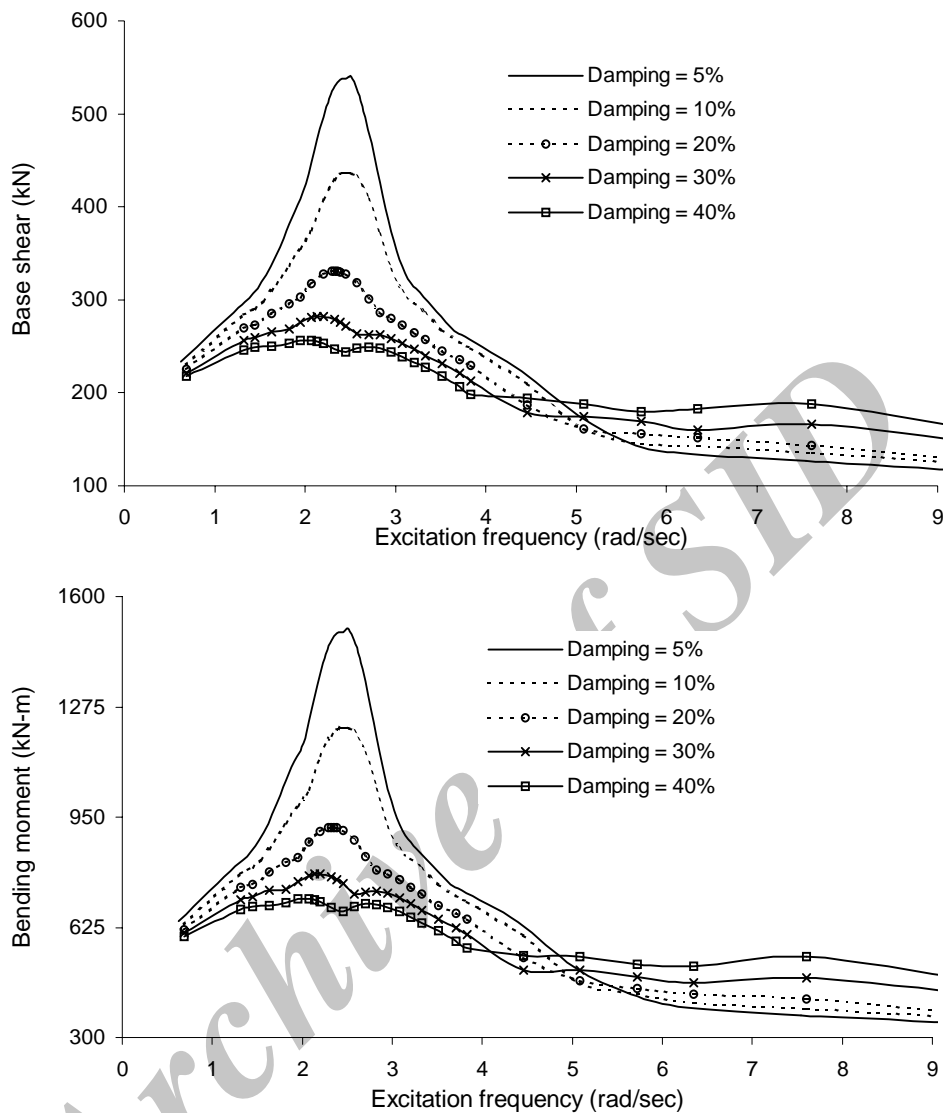


Figure 3. Variation of acceleration, base shear and bending moment of a base isolated four-storey space frame structure with excitation frequency

Figure 4 shows the variation of displacements with excitation frequency. It can be observed from Figure 4 that, the maximum top and base displacements occurs at 2.5 rad/sec for all isolation damping. It can also be observed from Figure 4 that, the top floor and base displacement decreases with the increase in isolation damping. However, for excitation frequency greater than 5.5 rad/sec the displacement curves for various isolation damping are nearly same. Thus the effectiveness of base isolation is dependent on the frequency characteristics of ground motion and isolation damping.



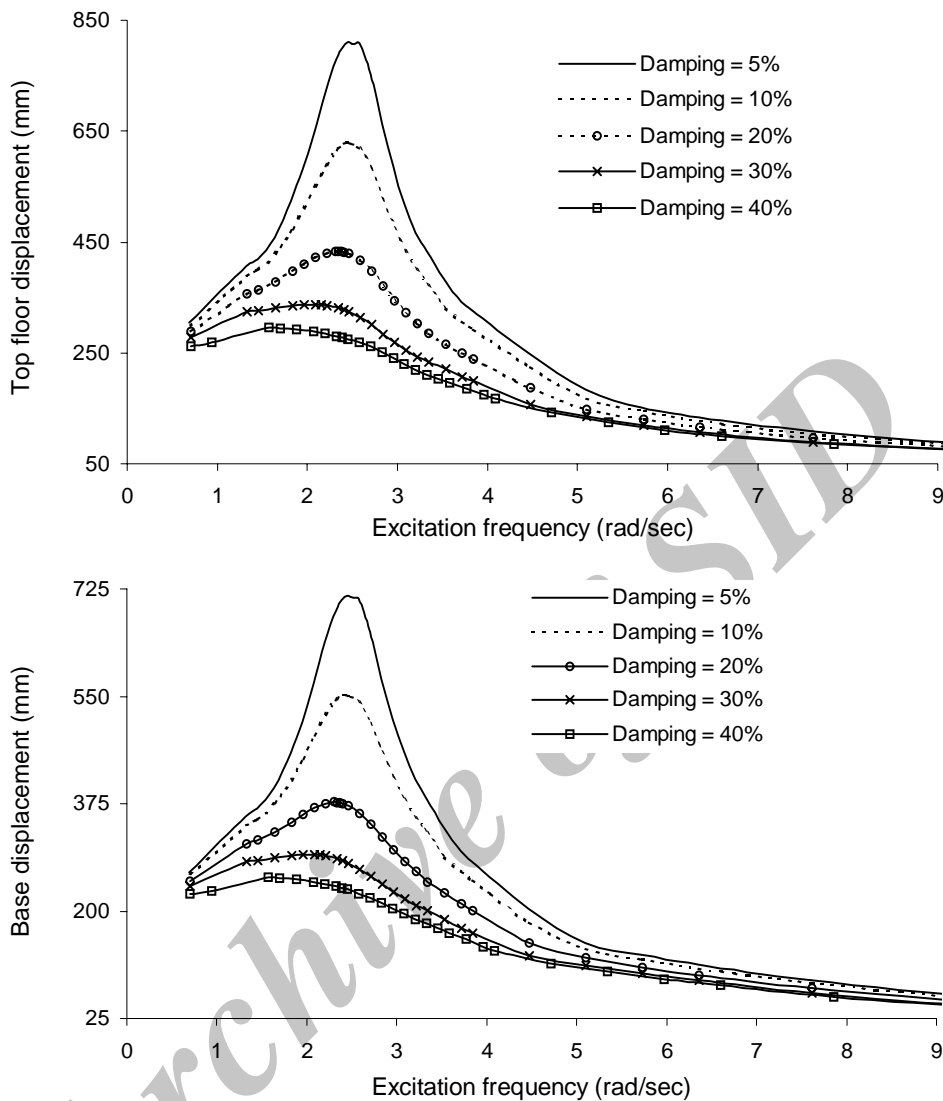


Figure 4. Variation of displacements of a base isolated four-storey space frame structure with excitation frequency

### 3.1.2 Effect of excitation frequency on the optimum isolation damping

The variation of response with isolation damping for a structure having fixed base time period equal to 0.75 sec and isolation period equal to 2.5 sec is shown in Figure 5. Damping is assumed to be 5% for superstructure. It can be observed from Figure 5 that as the isolation damping increases, the acceleration first decreases, thereby attaining a minimum value, and then increases with the increase of damping, indicating that there exists a value of damping in the isolation systems for which the acceleration of a given structural system attains a minimum value. This is the optimum isolation damping with respect to acceleration. Similar trend is observed in the case of base shear and bending moment. It can be seen from figure

that the optimum damping in isolation system for base shear and bending moment are almost same. But the optimum isolation damping for base shear and bending moment is different than that of the acceleration. It is also observed that the optimum damping decreases with the increase in excitation frequency. However, the top and base displacements decreases with the increase in isolation damping.

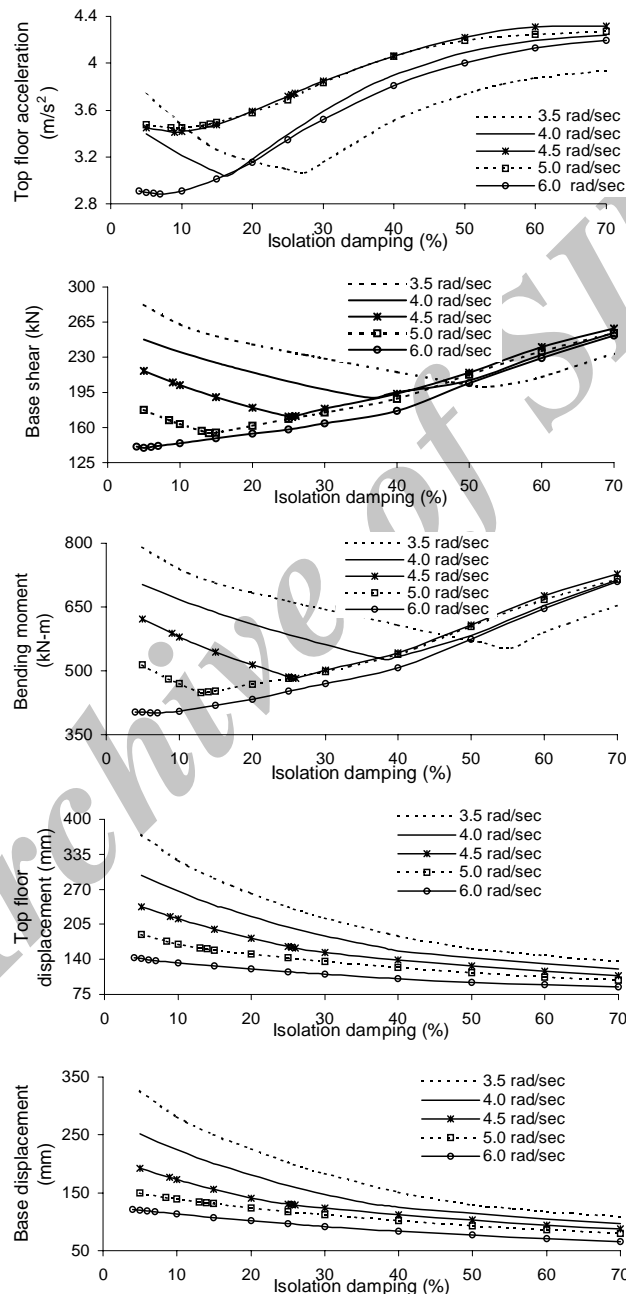


Figure 5. Variation of response of a base isolated four-storey space frame structure with isolation damping

### 3.1.3 Effect of isolation period on the optimum isolation damping

Figure 6 shows the effect of the base isolation period on the optimum isolation damping for a structure having fixed base time period equal to 0.75 sec and superstructure damping equal to 5%. The yield force and the post- to- pre yield stiffness ratio of the isolator are taken as 0.08 W and 0.2 respectively. The stiffness of the bearing is adjusted in order to get the required isolation period. It is seen from figures that the optimum isolation damping decreases with increase in the base isolation period. It is also observed that the optimum damping decreases with the increase in excitation frequency. Thus, an increase in the excitation frequency decreases the optimum isolation damping.

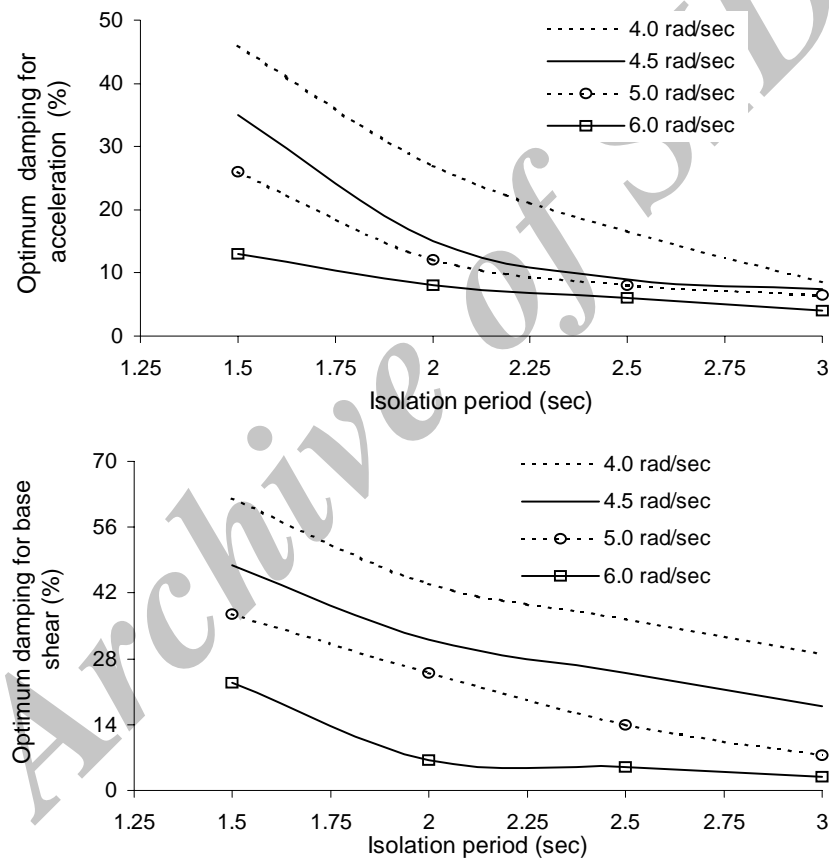


Figure 6. Variation of optimum damping with isolation period

### 3.1.4 Effect of superstructure time period on the optimum isolation damping

Figure 7 shows the variation of the optimum isolation damping against the time period of the superstructure. The various material and geometric properties considered for the study are shown in the table 1. The yield displacement of the isolator is taken as 2.5cm. This value of yield displacement provides (For  $R_t = R_c = 0.08 W$  and  $\gamma = 0.2$ ) a time period of the base

isolated structure in lateral direction as 2.5 sec based on post-yield stiffness of the isolator. Damping is assumed to be 5% for superstructure. It is observed from the figure that as the time period of the superstructure increases (in the range  $0.17 < T_s < 0.55 \text{sec}$ ), the optimum isolation damping increases.

Table 1. Material and geometric properties considered for the study

Number of storey	$T_s$ (sec)	Mass on each beam ( $\text{kN}\cdot\text{sec}^2/\text{m}^2$ )	b (m)	d (m)	h (m)	Size of beam (m)	Size of column (m)	E ( $\text{kN}/\text{m}^2$ )
1	0.172	4.2166	6	6	3.3	$0.3 \times 0.6$	$0.6 \times 0.6$	$2.24 \times 10^7$
2	0.353	4.2166	6	6	3.3	$0.3 \times 0.6$	$0.6 \times 0.6$	$2.24 \times 10^7$
3	0.547	4.2166	6	6	3.3	$0.3 \times 0.6$	$0.6 \times 0.6$	$2.24 \times 10^7$
4	0.75	4.2166	6	6	3.3	$0.3 \times 0.6$	$0.6 \times 0.6$	$2.24 \times 10^7$

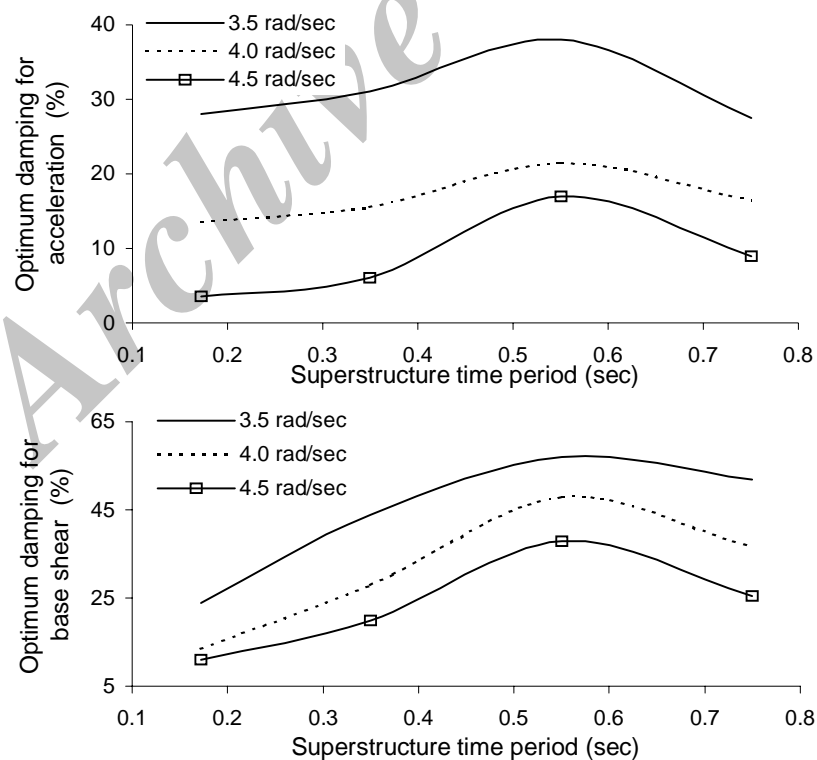


Figure 7. Variation of optimum damping with superstructure time period

However, for a further increase in the time period there is a decrease in the optimum isolation damping. Thus, the optimum isolation damping first increases and then decreases with the increase in the time period of the superstructure. It is also observed from the figure that, as the excitation frequency increases the optimum isolation damping decreases.

### 3.1.5 Effect of superstructure damping on the optimum isolation damping

In Figure 8 the variation of optimum isolation damping is plotted against the damping of the superstructure for  $T_s = 0.75$  sec and  $T_b = 2.5$  sec. It is observed from the figure that as the damping of the superstructure increases the optimum isolation damping decreases. Thus, an increase in the damping of the superstructure decreases the optimum isolation damping.

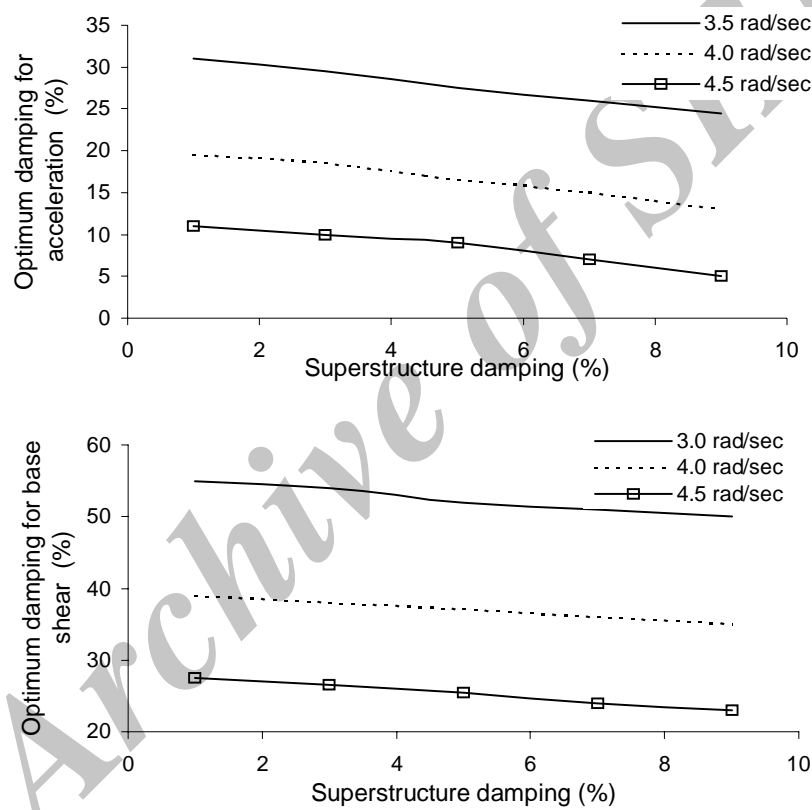


Figure 8. Variation of optimum damping with superstructure damping

### 3.2 Response of a four-storey space frame structure under real earthquake motion

The response of a multi-storey space frame structure resting on non-linear base isolation system, subjected to El Centro and Turkey earthquake excitation is studied. The top floor displacement, base displacement, top floor absolute acceleration, shear and bending moment at bottom column due to this loadings are computed at a time interval of 0.0004 seconds for a total period of 16.0 seconds. The time history response is shown in Figure 9 and Figure 10 for fixed base ( $T_s = 0.75$  sec) as well as base isolated ( $T_b = 2.5$  sec) structure. Damping is

assumed to be 5% and 10% for superstructure and bearing respectively. It can be seen from figure that there is a considerable reduction in the top floor absolute acceleration, base shear and bending moment due to isolation. The displacement at top and base of the isolated structure are almost same at all the time intervals. This indicates that the structure moves rigidly during earthquake.

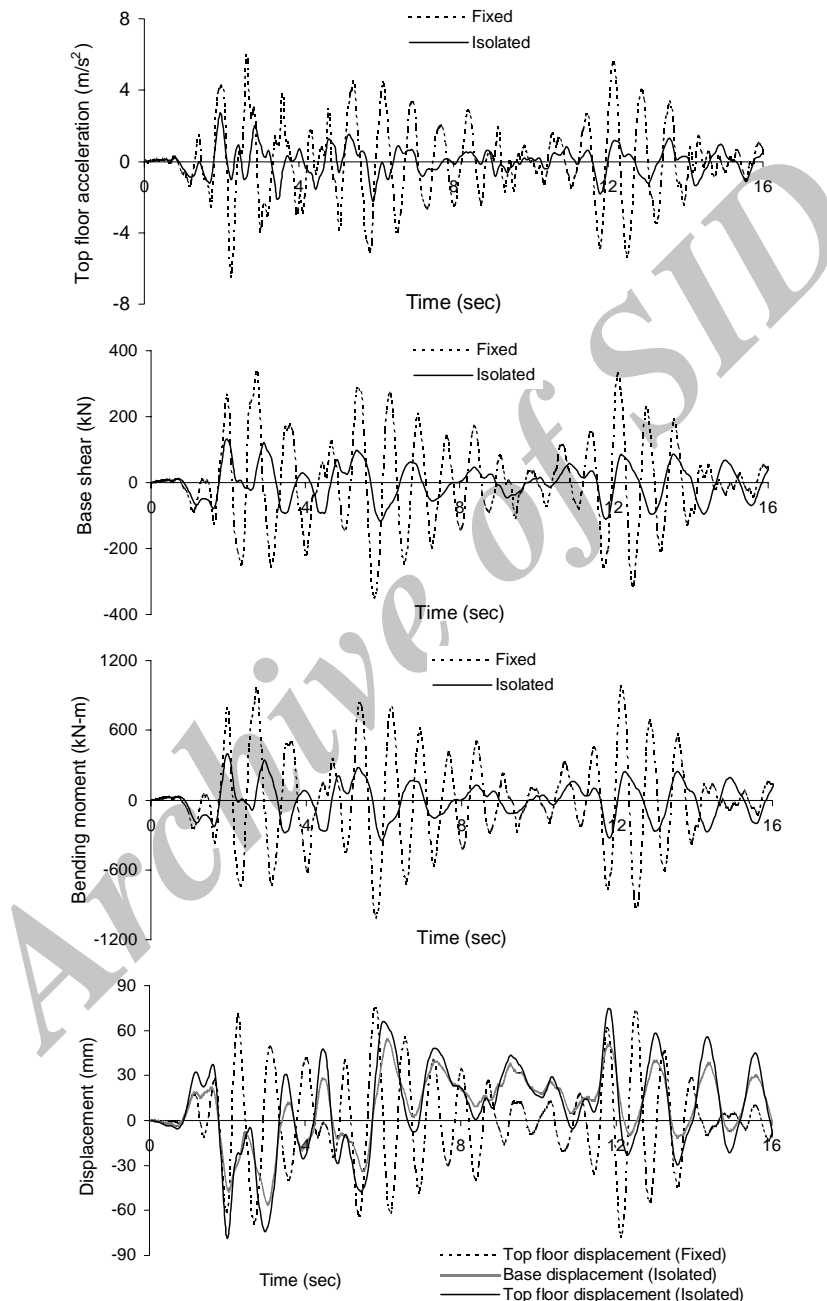


Figure 9. Response of base isolated four-storey space structure subjected to El-Centro earthquake ground motion

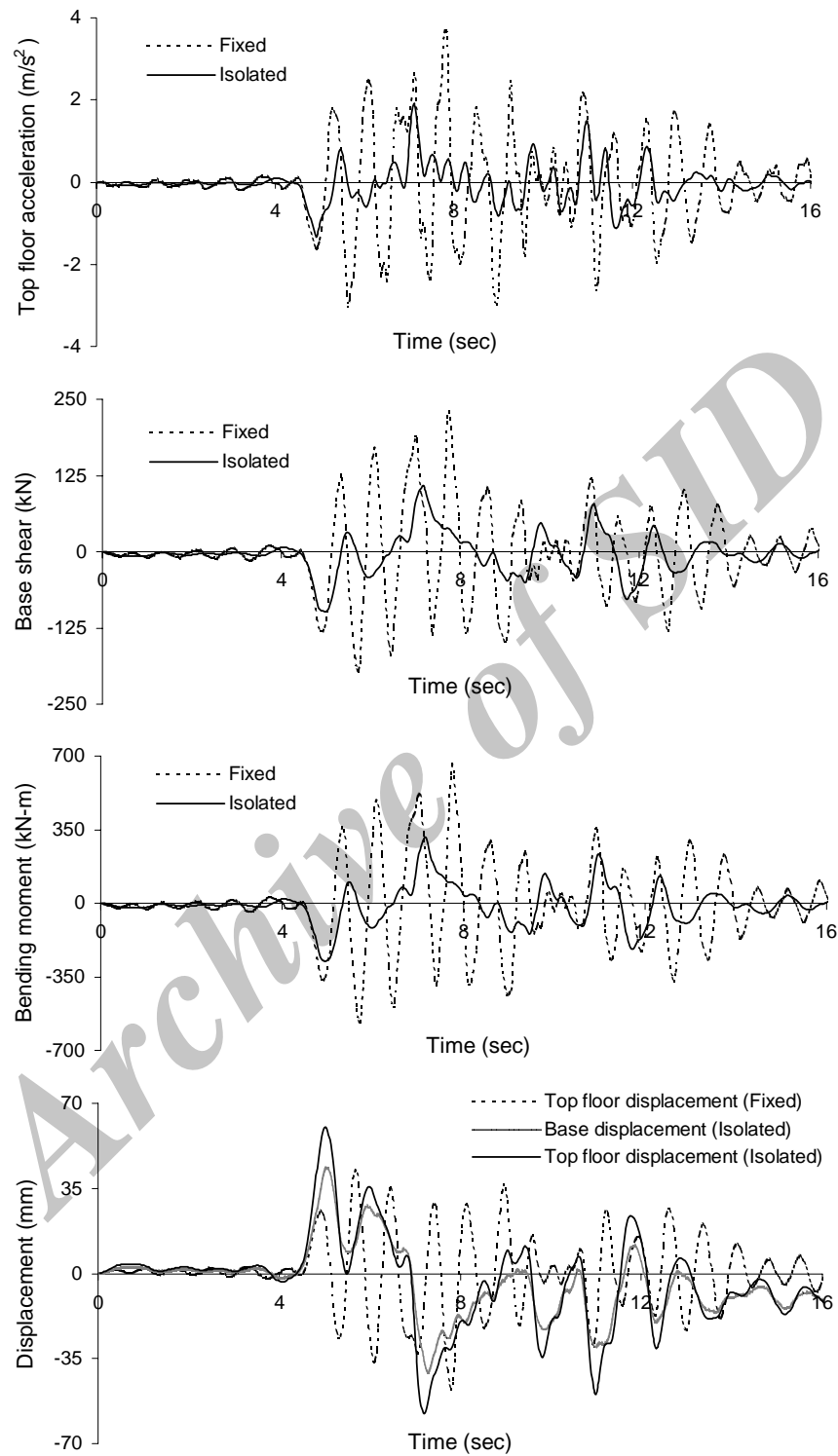


Figure 10. Response of base isolated four- storey space structure subjected to Turkey earthquake ground motion

#### 4. CONCLUSIONS

The response of a multi-story framed structure having six degrees of freedom at each node resting on non-linear base isolation system subjected to bi-directional harmonic ground motion, El Centro and Turkey earthquake ground motions are obtained. The effect of isolation damping and the excitation frequency on the response of a base isolated structure is investigated. The effect of excitation frequency, isolation period, superstructure time period and superstructure damping on the optimum isolation damping is also studied in this paper. The effectiveness of base isolation is studied by comparing the responses of base isolated structure with the response of the fixed base structure. The results of the study leads to the following conclusions:

1. The maximum acceleration, maximum base shear and maximum bending moment decreases due to isolation.
2. The displacement at top and base of the isolated structure are almost same at all the time intervals. This indicates that the structure moves rigidly during earthquake.
3. The effectiveness of base isolation is dependent on the frequency characteristics of ground motion and isolation damping.
4. The optimum damping in isolation system for base shear and bending moment are almost same. But the optimum isolation damping for base shear and bending moment is different than that of the acceleration.
5. The optimum isolation damping decreases with the increase in excitation frequency.
6. The optimum isolation damping decreases with the increase in the base isolation period.
7. The optimum isolation damping first increases and then decreases with the increase in the time period of the superstructure.
8. An increase in the damping of the superstructure decreases the optimum isolation damping.

#### REFERENCES

1. Kelly JM. Seismic base isolation: review and bibliography, *Soil Dynamics Earthquake Engineering*, **5**(1986) 202-16.
2. Buckle IG, Mayes RL. Seismic isolation: history, application and performance – A word overview, *Earthquake Spectra*, No. 2, **6**(1990) 161-202.
3. Bhasker R, Jangid RS. Experimental study of Base isolated Structures, *Journal of Earthquake Technology*, **38**(2001) 1-15.
4. Tsai H-C, Kelly JM. Seismic response of heavily damped base isolation systems, *Journal of Earthquake Engineering and Structural Dynamics*, **22**(1993) 633-45.
5. Inaudi J, Kelly JM. Optimum damping in linear isolation system, *Journal of Earthquake Engineering and Structural Dynamics*, **22**(1993) 583-98.
6. Jangid RS. Optimum damping in a non linear base isolation system, *Journal of Sound and Vibration*, No. 4, **189**(1996) 477-87.
7. Paz M. *Structural Dynamics*, CBS publishers, Delhi, 2001.